ICT IN EDUCATION PHYSICS

CORRELATION ANALYSIS OF DISTRICT HEATING PROCESSES USING TEMPERATURE CONTOUR APPROACH

ULDIS KANDERS

Riga Technical University, 6 Ezermalas St., Riga, Latvia, LV-1014, email: uldis.kanders@rtu.lv

Abstract

The article deals with correlation analysis of district heating (DH) processes using temperature contour (TC) approach based on investigation of the functional dependence between outdoor temperature, T_{out}, as the regressor, and DH process characterizing thermal or hydraulic parameters, P_{DH}, as the regresent, e.g., supply and return water temperature, T_S&T_R, as well as water mass flow, V. The time series of outdoor temperature, $\{T_{out'i}\}$, and supply water temperature, $\{T_{S'i}\}$, as well as T_{out}&T_S-scatter plots of ($T_{out'i}$; $T_{S'i}$)-data set have been examined more in details. It has been shown that using TC-approach one can additively construct linear regression models corresponding separately to each TC, and thereafter combining these models together and creating full regression curve for whole T_{out}&T_S-scatter plot. Also frequency distribution functions (FDF), $dFr(T_{out})$&$cFr(T_{out})$ and $dFr(T_S)$&$cFr(T_S)$, have been calculated for different size TC in order to explore corresponding ($T_{out'i}$; $T_{S'i}$)-data set immanent data structure. In the case of asymmetric TC it has been stated that ($T_{out'i}$; $T_{S'i}$)-points most likely are uniformly distributed along TC base-interval. However, along TC contiguous-interval ($T_{out'i}$; $T_{S'i}$)-points most likely are normally distributed.

Key words: *district heating, correlation analysis, frequency distribution function, regression model, temperature contour, scatter plot.*

Introduction

District heating (DH) systems provide heat for inhabitants of large cities and villages in a rational and economical manner. It is well known that heat from heat and power generating DH systems is cheaper than heat produced by individual low power boiler facilities. Large heat and power plants (CHP) producing heat for DH systems are generally equipped with high-efficiency combustion units reducing the greenhouse gases (GHG) emission into atmosphere. The GHG emission from small, local and dispersed sources using worse fuels is much higher than that from centralized large CHP. In Latvia district heating in large cities still dominates fortunately over local individual low power facilities. This is very important circumstance for reducing CO_2 emissions and for keeping atmosphere clean. Thus CHP as an area of utmost importance for Latvian economy provides heat for centralized heating systems which cover on average 70% of heat demand in cities of country. Therefore more than million citizens of our country use heat from heating networks which is produced by industrial and commercial heat of CHP as well as of municipal heat production plants as, e.g., of joint-stock Company "Rīgas Siltums".

Materials and Methods.

DH system consists of a heat producer as a heat source plant (HSP), of an external heat transmission network (HTN) built-up of thermo isolated pipes and hydraulic devices, as well as of many local heat substations (LHS) as internal heat distribution systems in which the heat from the DH supply water is transferred to the radiator circuit and to the hot water circuit of heat end user houses. Therefore one can split complicated DH system into three separate parts – HSP, HTN and LHS in order to reduce its complicity for investigation purposes. Thus HTN connects HSP with every LHS using both the supply water pipe and the return water pipe of the DH system. The input data for correlation analysis have been collected from HSP of DH system "Vecmilgravis" of city Riga as 6 thermal and 7 hydraulic DH process parameters, P_{DH}, time series as outdoor temperature, $\{T_{out'i}\}$, supply water temperature, $\{T_{S'i}\}$, heat load, $\{Q_i\}$, etc. of 4608 elements belonging to heating season (HS) 2008/2009 which endured 192 days from October till April or 4608 hours (h) long. DH process parameters, P_{DH}, time series were presented as data base of computer program "Microsoft® Office Excel 2003" containing 4608 records of 13 data fields (Kanders, Turlajs, 2009; Turlajs, Kanders, 2009). Thus the primary data set contains consequently about 60 thousand (59904 items) data field entries as parameter's 1-hour mean value. P_{DH}-time series have been graphically presented as HS-profiles respectively and compared one to each other. The time series of outdoor temperature, $\{T_{out'i}\}$, and supply water temperature, $\{T_{S'i}\}$, played important role in correlation analysis as the factorial variable called regressor and the response variable called regresent respectively. Moving correlation coefficient, R(mc), between HS-profiles of outdoor temperature, $T_{out'i}$, and supply water temperature,

$T_{S'i}$, has been calculated for different size of parameters' moving scatter vectors. In addition T_{out}&T_S-scatter plots of $(T_{out'i}; T_{S'i})$-points have been examined in order to create appropriate regression models for functional expressions between given regressor value and regresent mean value depending on regressor.

Results and Discussion

The time series of outdoor temperature, $\{T_{out'i}\}$, and supply water temperature, $\{T_{S'i}\}$, of DH system have been compared one to another and moving correlation coefficient, R(mc), has been calculated between heating season profiles (HSP) - T_{out}&T_S-HSP. There are tree types of the T_{out}&T_S-HSP smoothing extent considered in this paper. The first one is T_{out}&T_S-HSP built up of 1h-mean values (Fig.1), the second one is T_{out}&T_S-HSP built up of 24h-mean values (Fig.2), and however the third one is T_{out}&T_S-HSP built up of 168h-mean values of the DH parameters (Fig.3). All the T_{out}&T_S-HSP are calculated by 1h-time resolution that is high enough to reveal fine time structure in the much more as 1h-smoothed T_{out}&T_S-HSP as well. Smoothing is a pretty much used procedure to dampen or average out fluctuations in a time series to reveal a smooth component that reflects the systematic movement or some trend of the time series. One can be convinced that, e.g., outdoor temperature, T_{out}, oscillations are much more frequent as supply water temperature, T_S. By moving average method one can average out high frequency hourly oscillations shown in Fig.1 even during 1-day period (Fig.2), but much more smoothed tendencies one can reveal during 1-week period (Fig.3). Graphical presentation of T_{out}&T_S-HSP allow easy to compare DH parameters' HSP one to each other. In this connection it is easy to consider that daily (24h) and weekly (168h) T_{out}&T_S-HSP show very good synchronization between them. The 2nd-order parabolic regression lines, f_{out} & f_S, of the T_{out}&T_S-HSP manifest quite similar time dependence within whole HS. In addition the determination coefficients, R^2, of parabolic regression lines, f_{out} & f_S, are close enough even during whole HS despite of October an April when outdoor temperature is high and therefore supply temperature does not follow outdoor climatic changes at all. Within time period Dec-Jan-Feb the outdoor temperature is overall low therefore it is very important so that supply temperature follows outdoor climatic changes. It is not difficult to find correlation coefficient, R, between outdoor and supply temperatures, T_{out}&T_S, for this 3-months time period which is as high as 'R_{DJF}=-0,9053' or determination coefficient, R_{DJF}^2=0,8196. These coefficient values are considerably higher as those values as, R_{HS}=-0,8229 and R_{HS}^2=0,6772, for whole HS. The correlation coefficient, R, here above and below has been calculated by Pearson formula-

$$R_{xy} = \frac{N * \Sigma x_i y_i - (\Sigma x_i)(\Sigma y_i)}{\sqrt{N * \Sigma x_i^2 - (\Sigma x_i)^2} * \sqrt{N * \Sigma y_i^2 - (\Sigma y_i)^2}}\ , \qquad (1)$$

where 'x_i'- *i-th* element of the factorial variable or regressor *X* time series, observed in the subsequent time moments {... , *i-1, i, i+1,* ...}; 'y_i'- *i-th* element of the response variable or regresent *Y* time series, observed in the same subsequent time moments {... , *i-1, i, i+1,* ...}; '*N*' – the number of pairs $(x_i; y_i)$ of variables *X&Y*. In the case of daily (24h) and weekly (168h) T_{out}&T_S-HSP it has been respectively found that R_{DJF}=-0.9320 and R_{DJF}^2=0,8690 for daily mean values, as well as R_{DJF}=-0,9274 and R_{DJF}^2=0,8601 for weekly mean values. The outdoor and supply temperatures have very similar daily, T_{out}&T_S-HSP(24h), and weekly, T_{out}&T_S-HSP(168h), time dependencies and high values of the pair correlation coefficient, R, in general. Detailed information about pair correlation coefficient, R, concerning separate HS-month is given in Table 1 below. The month's R-values in Table 1 are sorted descending by R^2-value showing January as the month in which correlative bond between DH parameters T_{out}&T_S is the strongest one while October R-value indicates the weakest correlative bond between T_{out}&T_S.

Table 1.

DH parameters' T_{out}&T_S pair correlation within separate month of heating season.

Month	R	R^2
Whole HS: Oct-Apr	-0.822861	0.6771
January	-0.943981	0.8911
February	-0.912140	0.8320
December	-0.847054	0.7175
November	-0.751332	0.5645
March	-0.695557	0.4838
April	-0.280713	0.0788
October	-0.067082	0.0045

As correlation coefficient, R, manifests strong correlative bond between DH parameters T_{out}&T_S, then it is good reason for building-up regression models and seeking functional dependencies between T_{out}&T_S that is shown in Fig.4-7 below. In addition moving correlation coefficient, R(mc), between outdoor and supply temperatures, T_{out}&T_S, has been calculated using different size of DH parameters' moving scatter vectors. The use of moving scatter vectors on daily basis, i.e., on 24-point basis was not reasonably because calculated R(mc)-values present very strong oscillations between -1 and +1 while moving scatter vectors on weekly basis (Fig.1 & Fig.3) and on 2-weeks basis (Fig.2) were good enough in order to assess correlation between DH parameters more in details. R(mc) curves in all the cases (Fig.1, Fig.2 & Fig.3) demonstrate not only overall but even differentially strong correlation between outdoor and supply temperatures, T_{out}&T_S, with the exception of some short time intervals in which moving correlation coefficient, R(mc), absolute values fall below0.75-value.

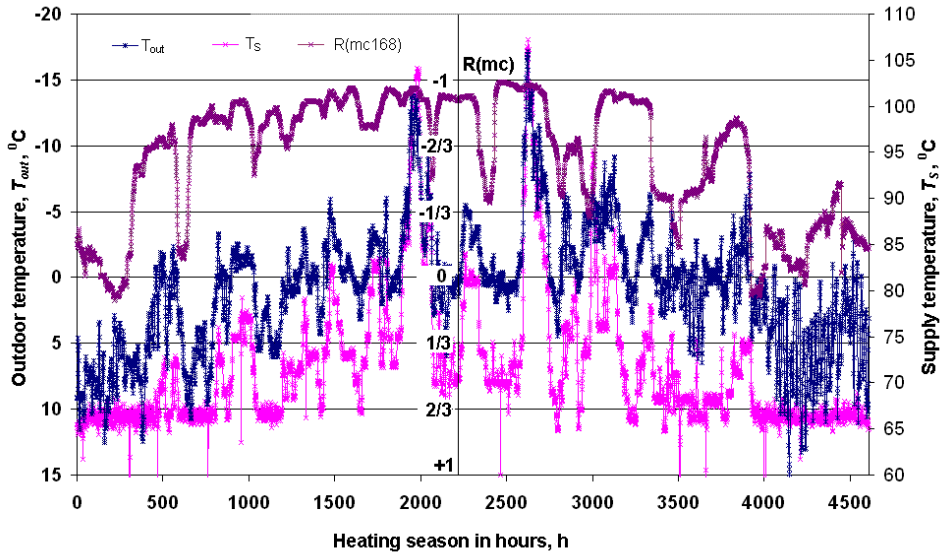

Fig.1. Outdoor and supply temperature heating season profiles (HSP) - T_{out}&T_S-HSP as 1h-mean values with 1h-time resolution. T_{out}&T_S-HSP correlation assessment by means of moving correlation coefficient, R(mc168), on 168-point basis with 1h-time resolution.

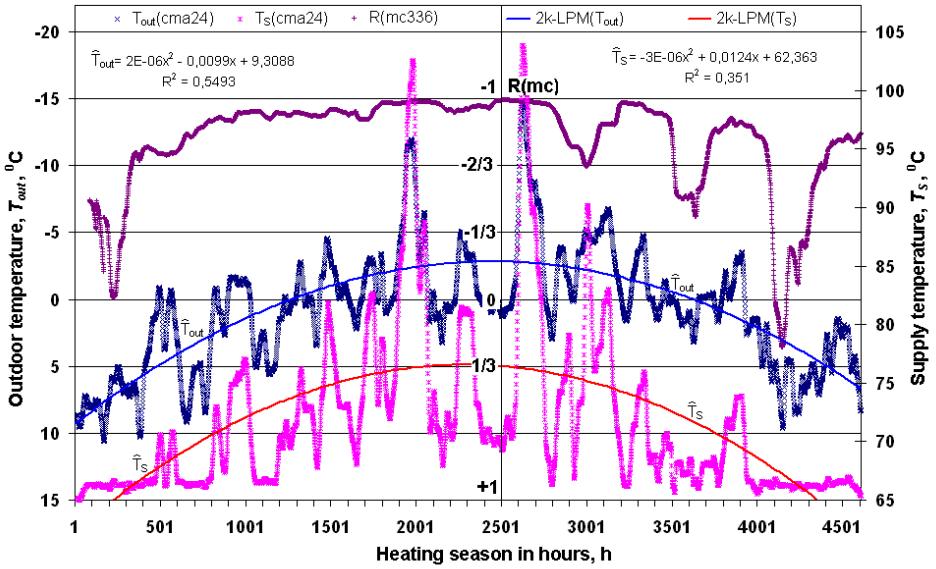

Fig.2. Outdoor and supply temperature heating season profiles (HSP) - T_{out}&T_S-HSP as 24h-mean values with 1h-time resolution. Parabolic regression curves and equations for T_{out}&T_S-HSP. T_{out}&T_S-HSP correlation assessment by means of moving correlation coefficient, R(mc336), on 336-point basis with 1h-time resolution.

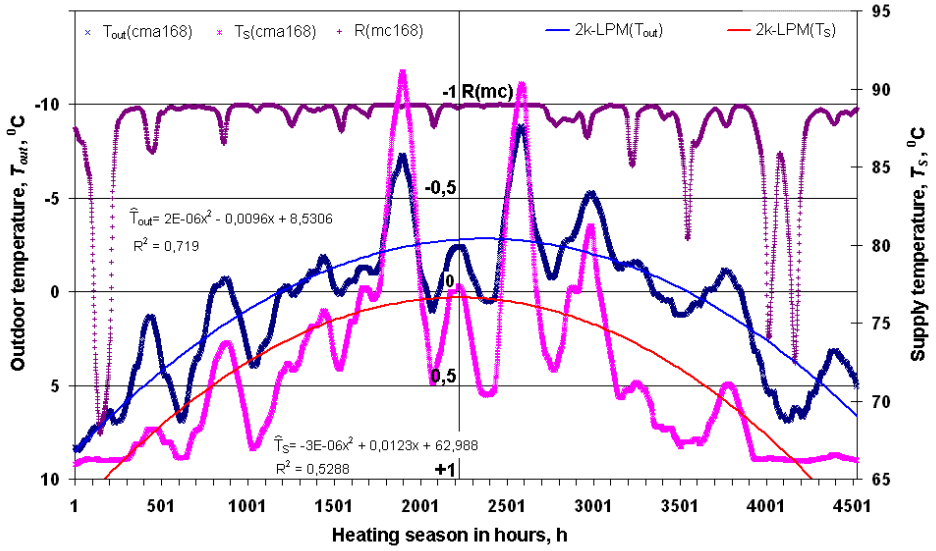

Fig.3. Outdoor and supply temperature heating season profiles (HSP) - T_{out}&T_S-HSP as 168h-mean values with 1h-time resolution. Parabolic regression curves and equations for T_{out}&T_S-HSP. T_{out}&T_S-HSP correlation assessment by means of moving correlation coefficient, R(mc168), on 168-point basis with 1h-time resolution.

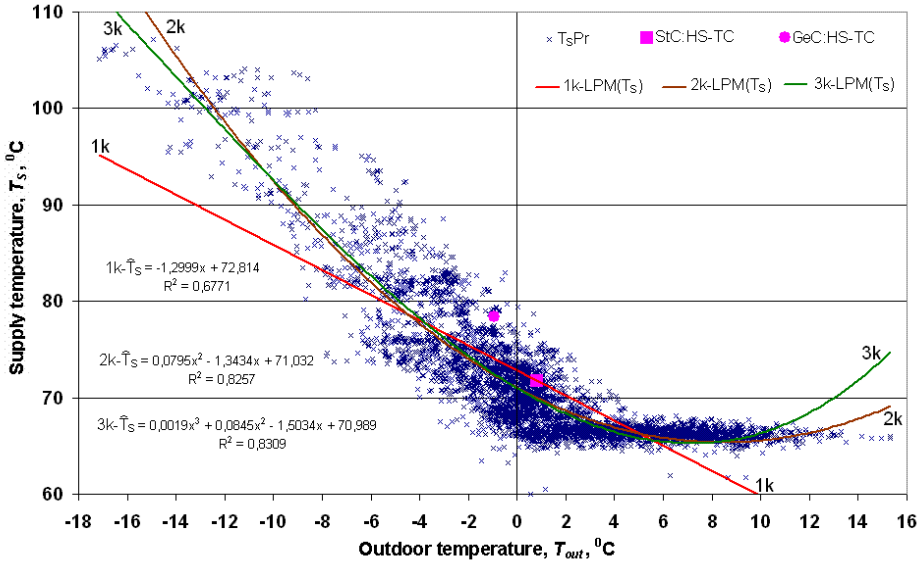

Fig.4. Outdoor and supply temperature T_{out}&T_S-scatter plot corresponding to whole heating season (HS) and three regression curves '1k', '2k' and '3k' with respect to linear polinomial regression models (LPM) concerning HS-TC. Statistical centre (StC) of the HS-TC is defined as averaged coordinates of ($T_{out'i}$; $T_{S'i}$)-point data set, whereas the geometrical centre (GeC) of the HS-TC is estimated as averaged coordinates of MIN&MAX values of ($T_{out'i}$; $T_{S'i}$)-point data set.

Outdoor and supply temperature T_{out}&T_S-scatter plot (Fig.4) corresponds to whole heating season (HS) from October till April hence the plot contains 4608 ($T_{out'i}$; $T_{S'i}$)-points. Linear least squares regression is by far the most widely used modeling method to fit a mathematical model to experimentally obtained data. There three types, 'NonPM(1)', 'NonPM(2)' and 'nk-LPM', of regression models, as well as six different orders of polynomial model 'nk-LPM', from '1k-LPM' up to '6k-LPM', of regression equations in Fig.5 are discussed in order to show how much sensitive is the choice of model with respect to determination coefficient. Thus two non-parametric models 'NonPM(1)' and 'NonPM(2)' which will be discussed below in Fig.8&Fig.9 manifests the highest determination coefficient, R^2, within whole HS in comparison with 'nk-LPM' type models shown in Fig.4. With this respect one can examine three linear polynomial models (LPM) '1k-LPM(T_S)', '2k-LPM(T_S)' and '3k-LPM(T_S)' as polynomial equations of 1st-, 2nd- and 3rd-order (Fig.4) which are built-up using linear least squares method. In the same way regression equations '4k-LPM(T_S)', '5k-LPM(T_S)' and '6k-LPM(T_S)' have been created and corresponding determination coefficients estimated. As it is well definable from Fig.5 then determination coefficient, R^2, go up rapidly by increasing LPM-equation's order from '1k' to '2k' then reaching quickly saturation. In the case of the T_{out}&T_S-scatter plot corresponding to 744 ($T_{out'i}$; $T_{S'i}$)-point data set of January determination coefficient's, R^2, values are high even at 1st-order LPM equation '1k-LPM(T_S)'. Therefore dependence of determination coefficient on LPM equation's order is weaker and saturation effect is more distinguished.

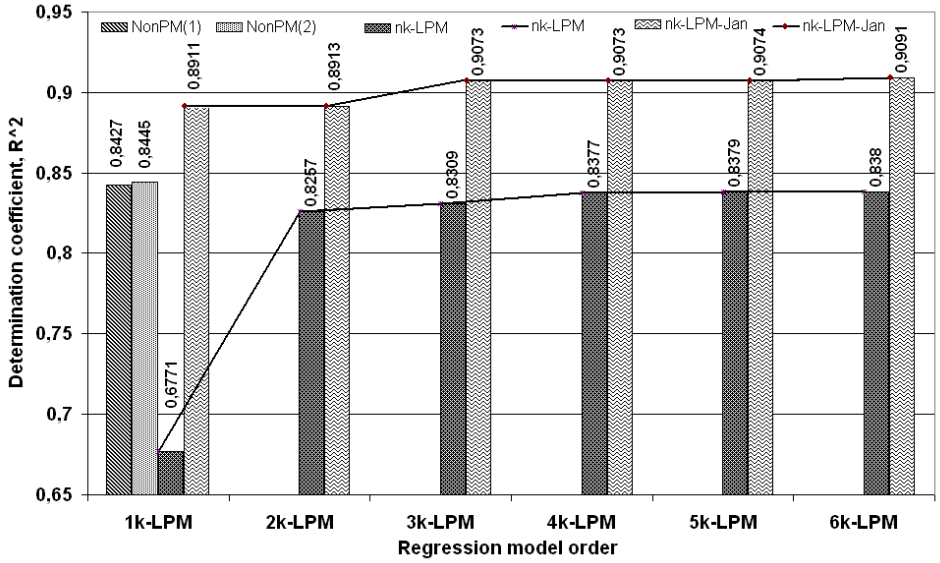

Fig.5. Determination coefficient, R^2, dependence on regression model type and on regression equation order.

Essence of temperature contour (TC) approach is based on merging graphical representation of T_{out}&T_S-scatter plot of ($T_{out'i}$; $T_{S'i}$)-point data set with statistical analysis of the same data set. Therefore one can imagine statistically defined ($T_{out'i}$; $T_{S'i}$)-point data set in T_{out}xT_S–coordinates as geometrical figure called temperature contour (TC). In the case of whole HS the ($T_{out'i}$; $T_{S'i}$)-point data set form HS-TC. Thus TC as geometrical and statistical object has simultaneously both geometrical and statistical properties. TC geometrical properties as width, height, or geometrical centre (GeC) have been estimated using MIN&MAX values and range of ($T_{out'i}$; $T_{S'i}$)-point coordinates while TC statistical properties as statistical centre (StC) and central tendencies are defined as mean, median and mode of ($T_{out'i}$; $T_{S'i}$)-point coordinates. Hence correlation analysis of district heating (DH) processes becomes more graphic, more visual and more demonstrative using TC approach. In addition TC approach helps split large ($T_{out'i}$; $T_{S'i}$)-point data sets into smaller portions, namely, sub-TC (Fig.6) and build-up partial regression models providing effective investigation of the functional dependence between outdoor temperature, T_{out}, as the regressor, and DH process characterizing thermal or hydraulic parameters, P_{DH}, as the regresent, e.g., supply and return water temperature, T_S&T_R, as well as water mass flow, V. So HS-TC representing large ($T_{out'i}$; $T_{S'i}$)-point data set in regard to whole HS can be divided into several smaller sub-TC_j with respect that union of all the sub-TC_j is equal to HS-TC (Fig.6&Fig.7) -

$$sub\text{-}TC_1 \bigcup sub\text{-}TC_2 ..... \bigcup sub\text{-}TC_j \bigcup ... \bigcup sub\text{-}TC_M = HS\text{-}TC; \quad (2)$$

$$\sum_{j=1}^{M} N_j = N \text{ , where } j=1, 2, 3, \ ..., M; \quad (3)$$

Parameter, M, is a number of sub-TC_j that in the case of T_{out}&T_S-scatter plot considered above in Fig.6 are as many as 34 vertical asymmetric sub-TC_j of the HS-TC, denoted here as V('j')-TC. Each of these V('j')-TC has 1-centigrade base-interval along T_{out}–axis and size, N_j, corresponding to the number of ($T_{out'i}$; $T_{S'i}$)-points included TC. Each sub-TC_j, has its own label, 'j', e.g., '-17' for j=1 and '16' for j=34. The label, 'j', of the V('j')-TC is derived from its base-interval's upper limit.

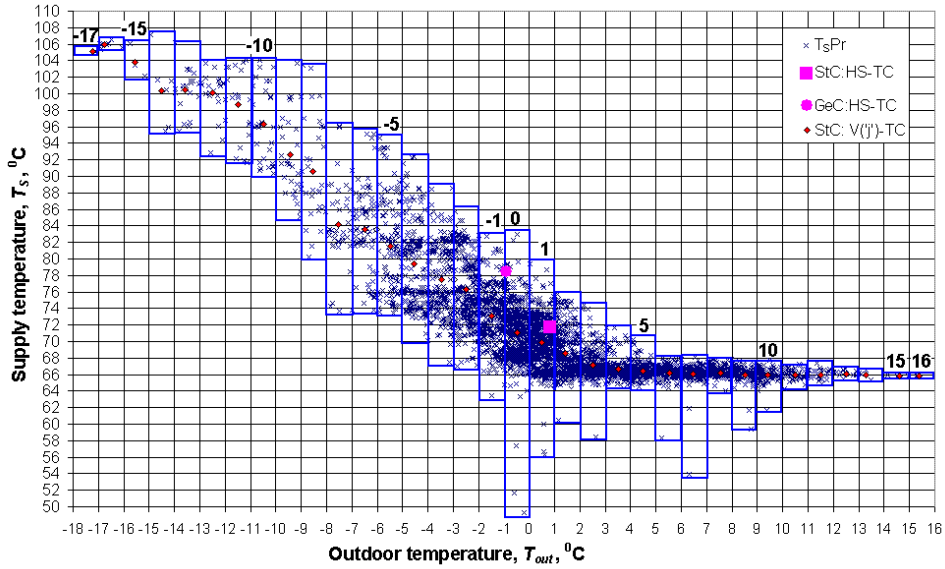

Fig.6. Outdoor and supply temperature T_{out}&T_S-scatter plot corresponding to whole heating season - HS-TC which is divided into 34 vertical asymmetric sub-TC_j of the HS-TC, V('j')-TC, having 1-centigrade base-interval and size N_j. Each sub-TC_j, has its own label, e.g., '-17' for j=1 and '16' for j=34 and its own StC. The label, 'j', of the V('j')-TC is derived from its base-interval's upper limit.

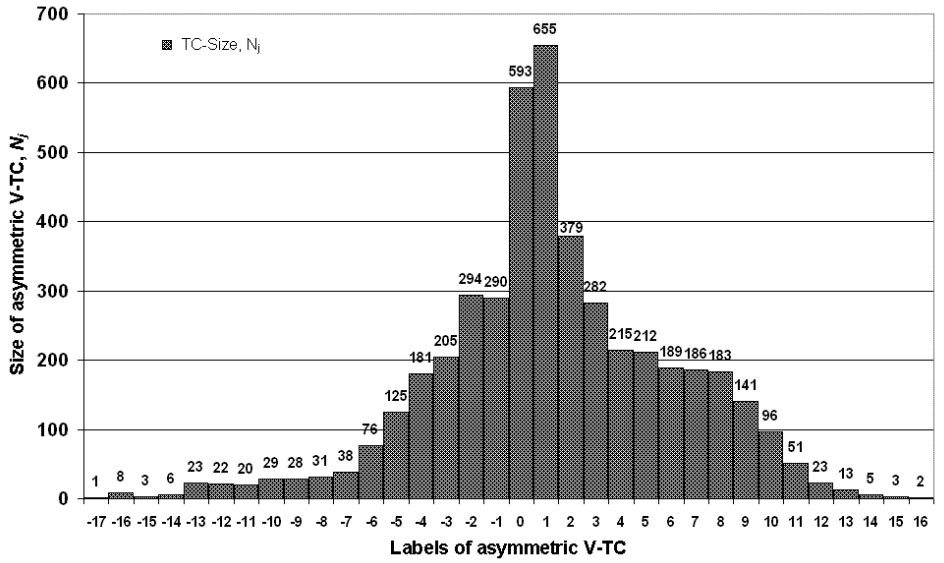

Fig.7. Distribution of all the 34 V('j')-TC corresponding to their 1-centigrade base-intervals with respect to outdoor temperature. The V('j')-TC are built-up as asymmetric sub-TC_j of the HS-TC and their size is determined by the number of ($T_{out'i}$; $T_{S'i}$)-points included in them. The label, 'j', of the V('j')-TC is created from the corresponding base-interval upper limit.

Histogram in Fig.7 can be considered either as differential frequency distribution function, *dFDF(T_{out})*, of outdoor temperature, T_{out}, or TC size distribution of all the 34 V('j')-TC corresponding to their 1-centigrade base-

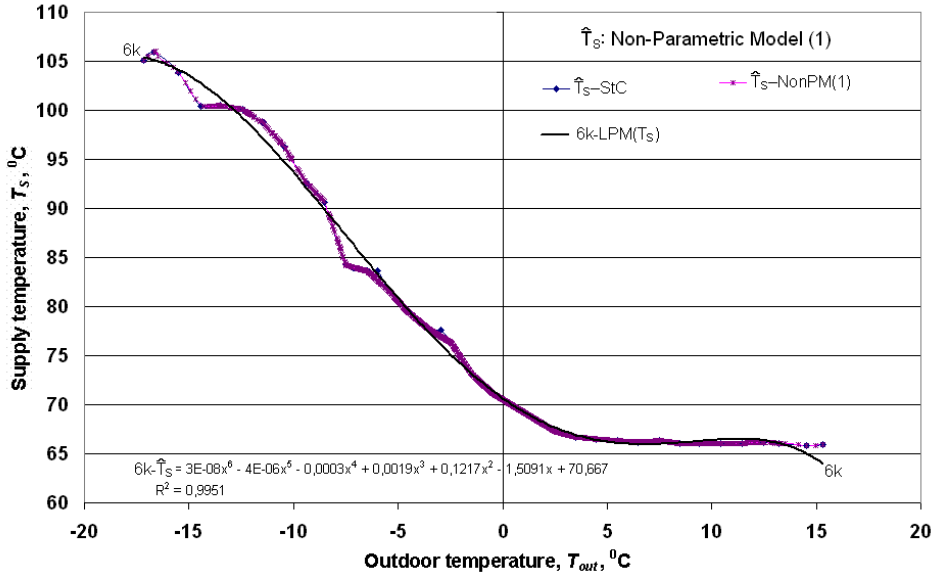

Fig.8. Regression models' backbone curve 'T_S-StC' - spline interpolation curve through statistical centres (StC) of all the 34 V('j')-TC. Non-parametric regression model 'T_S-NonPM(1)' for T_{out}&T_S-scatter plot of HS-TC built-up as linear interpolation between StC of asymmetric V('j')-TC. 6th-order trendline '6k-LPM(T_S)' for regression model 'T_S-NonPM(1)'.

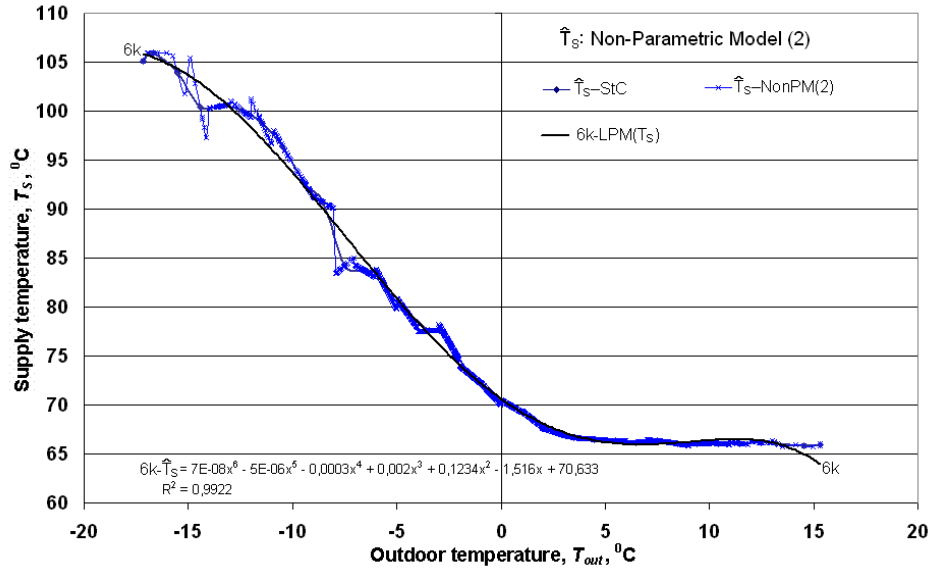

Fig.9. Regression models' backbone curve 'T_S-StC' - spline interpolation curve through statistical centres (StC) of all the 34 V('j')-TC. Non-parametric regression model 'T_S-NonPM(2)' for T_{out}&T_S-scatter plot of HS-TC built-up as linear combination of 1st-order regression line segments corresponding to each V('j')-TC. 6th-order trendline '6k-LPM(T_S)' for regression model 'T_S-NonPM(2)'.

intervals with respect to outdoor temperature. The V1-TC with base-interval $T_{out}\in[0; +1]$ is the biggest one because contains the maximum of 655 ($T_{out'i}$; $T_{S'i}$)-points whereas the smallest V(-17)-TC with base-interval $T_{out}\in[-18; -17]$ contains only one ($T_{out'i}$; $T_{S'i}$)-point. All the 34 V('j')-TC from V(-17)-TC up to V(16)-TC contain

together 4608 ($T_{out'i}$; $T_{S'i}$)-points that are as many as the HS-TC size. Thus, the regression model of the T_{out}&T_S-scatter plot surrounded by HS-TC can be set up additively, combining separate regression models associated with appropriate V('j')-TC (Fig.8&Fig.9). Each asymmetric V('j')-TC has its own StC_j as it was mentioned above in regard to the HS-TC in Fig.4. Thus, e.g., V(0)-TC has StC_0 with coordinates (-0,4982; 71,1702) which are obtained by averaging 593 ($T_{out'i}$; $T_{S'i}$)-point coordinates included in V(0)-TC. V(1)-TC next to the V(0)-TC has StC_1 with coordinates (0,4763; 69,9102) corresponding to averaged 655 ($T_{out'i}$; $T_{S'i}$)-point coordinates, and so on. So there are 34 StC_j of the 34 V('j')-TC which can be connected in different way in order to create non-parametric regression line for the T_{out}&T_S-scatter plot. There are three types of interpolation considered in Fig.8&Fig.9 how 34 StC_j of V('j')-TC are to be linked by line segment, by spline and by local regression line within asymmetric V('j')-TC intersecting its StC_j ('StC: V('j')-TC points in Fig.6). In the case of a linear line segment interpolation here denoted as 'NonPM(1)' one has to create 'M-1' linear equations for linking each pair of two closest StC_j. Thereafter regression line '$\hat{T}_S$-NonPM(1)' has been calculated corresponding to each $T_{out'i}$-value. It means to estimate 4608 ($T_{out'i}$; $\hat{T}_{S'i}$)-points for regression line '$\hat{T}_S$-NonPM(1)' shown in Fig.8. Determination coefficient, R^2, between vectors {$T_{S'i}$} and {$\hat{T}_{S'i}$} reaches as high value as '0.8427'. In principle the regression line '$\hat{T}_S$-NonPM(1)' is continuous but broken line in local StC_j-points by definition therefore in these StC_j-points does not exist 1st-order derivative. On the contrary the cubic spline interpolation gives smoothed continuous regression line having 1st-order derivative at each data point. The cubic spline interpolation giving curves 'T_S-StC' called here backbone curves in Fig.8&Fig.9 is mathematically more complicated method as a simple linear interpolation between StC_i-points. Despite of this it is easy to be convinced that there is very negligible difference between regression lines '$\hat{T}_S$-NonPM(1)' and '$\hat{T}_S$-StC' in Fig.9. Moreover, one can obtain more smoothed trendline '6k-LPM(T_S)' for the regression line '$\hat{T}_S$-NonPM(1)' and other trendline for cubic spline '$\hat{T}_S$-StC' not shown in Fig.8&Fig.9, as well as compare corresponding trendlines' equations (4) and (5) respectively:

$$\begin{cases} \hat{T}_S = 3E\text{-}08\, T_{out}\text{^}6 - 4E\text{-}06\, T_{out}\text{^}5 - 0{,}0003 T_{out}\text{^}4 + 0{,}0019 T_{out}\text{^}3 + 0{,}1217 T_{out}\text{^}2 - 1{,}5091 T_{out} + 70{,}667; \\ R\text{^}2 = 0{,}9951 \text{ for regression line '}\hat{T}_S\text{-NonPM(1)'}; \end{cases} \quad (4)$$

and

$$\begin{cases} \hat{T}_S = 5E\text{-}07 T_{out}\text{^}6 + 2E\text{-}06 T_{out}\text{^}5 - 0{,}0004 T_{out}\text{^}4 + 0{,}0007 T_{out}\text{^}3 + 0{,}1305 T_{out}\text{^}2 - 1{,}4696 T_{out} + 70{,}644; \\ R\text{^}2 = 0{,}9961 \text{ for regression line '}\hat{T}_S\text{-StC'}. \end{cases} \quad (5)$$

The trendlines' equations (4) and (5) differ very slightly that is negligible in a case of their graphic representation. The third type of interpolation is based on the drawing of a local 1st-order regression line through each StC_j within a range of the V('j')-TC. In this case regression line '$\hat{T}_S$-NonPM(2)' in Fig.9 is a piecewise continuous line within a range of each V('j')-TC. The regression line '$\hat{T}_S$-NonPM(2)' undergoes 'M-1' disruptions in the juncture points of the V('j')-TC's base-intervals. It is worth to mention that such a piecewise continuous regression line '$\hat{T}_S$-NonPM(2)' demonstrates the highest determination coefficient, R^2=0,8445, in comparison with other regression models built-up by linear least square method shown in Fig.4 or by different interpolation procedures between StC_j-points. The regression line '$\hat{T}_S$-NonPM(2)' denoted here as non-parametric model of T_{out}&T_S-scatter plot like other non-parametric models '$\hat{T}_S$-NonPM(2)' and 'T_S-StC' obtained by asymmetric TC approach manifest in principle higher determination coefficient, R^2, as parametric 'nk-LPM' type models. One can obtain more smoothed trendline '6k-LPM(T_S)' for the regression line '$\hat{T}_S$-NonPM(2)' and other trendline '$\hat{T}_S$-6k-LPM' for T_{out}&T_S-scatter plot of HS-TC, as well as compare corresponding trendlines' equations (6) and (7) respectively:

$$\begin{cases} \hat{T}_S = 7E\text{-}08 T_{out}\text{^}6 - 5E\text{-}06 T_{out}\text{^}5 - 0{,}0003 T_{out}\text{^}4 + 0{,}002 T_{out}\text{^}3 + 0{,}1234 T_{out}\text{^}2 - 1{,}516 T_{out} + 70{,}633; \\ R\text{^}2 = 0{,}9922 \text{ for regression line '}\hat{T}_S\text{-NonPM(2)'}; \end{cases} \quad (6)$$

and

$$\begin{cases} T_S = 8E\text{-}08T_{out}\text{^}6 - 5E\text{-}06T_{out}\text{^}5 - 0{,}0003T_{out}\text{^}4 + 0{,}002T_{out}\text{^}3 + 0{,}1236T_{out}\text{^}2 - 1{,}5159T_{out} + 70{,}632; \\ R\text{^}2 = 0{,}8380 \text{ for } T_{out}\&T_S\text{-scatter plot of HS-TC.} \end{cases} \quad (7)$$

All the trendlines' equations (4)-(5)-(6)-(7) differ very slightly that is negligible in a case of their graphic representation. Deeper and more detailed picture about ($T_{out'i}$; $T_{S'i}$)-point data set structure has been derived by calculating their frequency distribution functions (FDF) with respect to HS-TC (Fig.10& Fig.11).

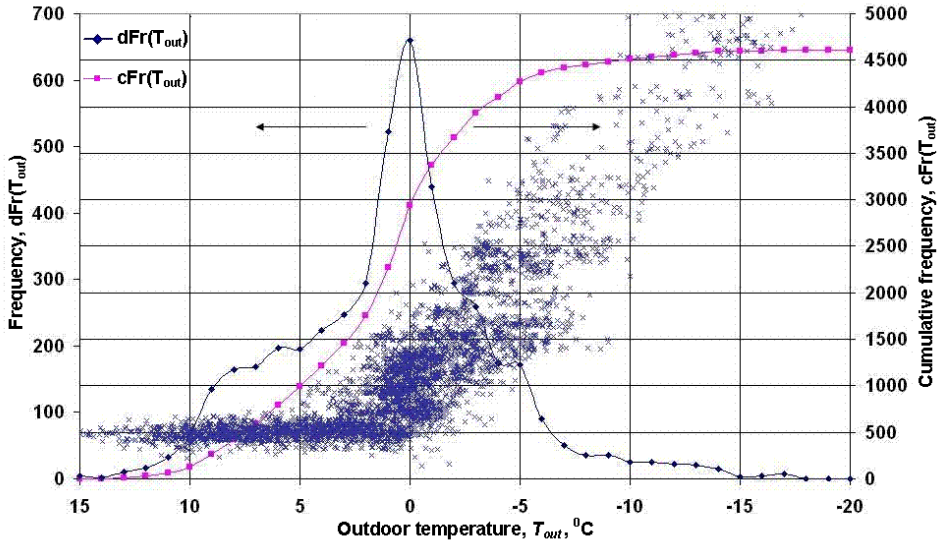

Fig.10. Differential and cumulative frequency distribution functions, $dFr(T_{out})$ & $cFr(T_{out})$, of the outdoor temperature, T_{out}, with the $T_{out}\&T_S$-scatter plot of HS-TC in the background.

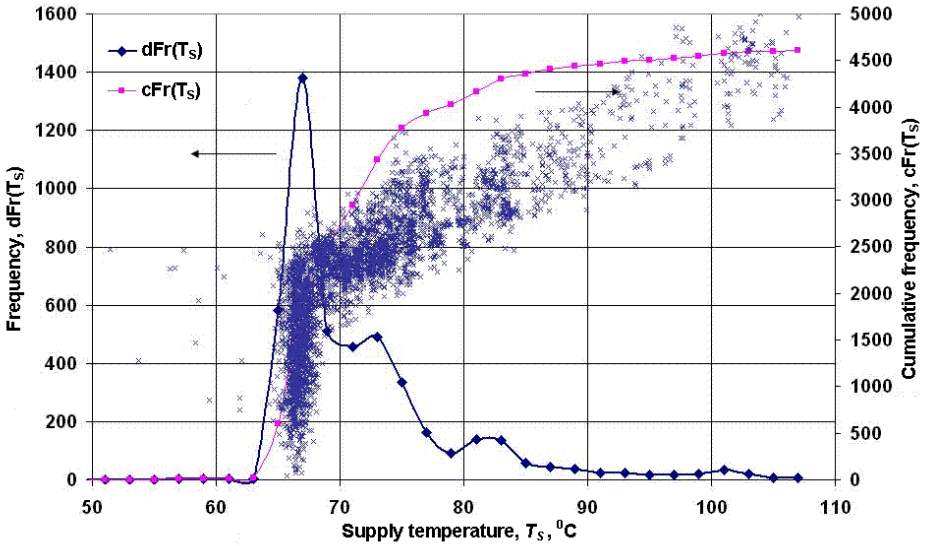

Fig.11. Differential and cumulative frequency distribution functions, $dFr(T_S)$ & $cFr(T_S)$, of the outdoor temperature, T_S, with the $T_{out}\&T_S$-scatter plot of HS-TC in the background.

On the basis of empirical FDF was developed temperature spectroscopy of such DH parameters as outdoor temperature, T_{out}, supply and return water temperature, T_S&T_R, etc. Differential and cumulative (integral) FDF, namely, dFr(T_{out})&cFr(T_{out}) in Fig.10 and dFr(T_S)&cFr(T_S) in Fig.11 corresponding to HS-TC have been calculated at least in 3%-high resolution because temperature class intervals of 1- and 2-degrees in length were used for T_{out}–axis and T_S–axis respectively. Vertical Y-axis on the left hand side of Fig.10& Fig.11 relates to differential frequency, dFr, while other vertical Y-axis on the right hand side relates to cumulative frequency, cFr. T_{out}&T_S-scatter plot of HS-TC in the background of the FDF in Fig.10& Fig.11 allows comparing peaks, local maximums and shoulders of FDF with ($T_{out'i}$; $T_{S'i}$)-point spatial density. One can be convinced that peaks and local maximums correlate very well with with ($T_{out'i}$; $T_{S'i}$)-point spatial density spots. It is worth to mention that outdoor temperature, T_{out}, is distributed unequally pretty much because, e.g., interval $T_{out}\in$[-2; +2] having only 4-centigrade length of 33-centigrade T_{out}–scale contains 1920 ($T_{out'i}$; $T_{S'i}$)-points of HS-TC, i.e., 42% of HS-TC's size. In a similar manner a such kind temperature spectroscopy has been developed relating to asymmetric V('j')-TC of different type and different size. Such approach was applied to investigate peaks and local maximums of FDF more in details. Moreover, such asymmetric TC approach was used to demarcate comparatively small areas of the complete T_{out}&T_S-scatter plot and to investigate local ($T_{out'i}$; $T_{S'i}$)-point data set temperature fluctuations in circumstances where one of the DH-parameter, outdoor temperature, T_{out}, or supply water temperature, T_S, is greatly limited by small size of asymmetric TC base-interval, but other one may fluctuate without any restrictions.

In such a way it was possible to clarify the large-scale fluctuations by $33{,}40^0$C amplitude of the supply temperature, T_S, while outdoor temperature, T_{out}, was restricted within TC base-interval $T_{out}\in$[-1; 0] in the case of V(0)-TC. In addition to that two more other places of the complete ($T_{out'i}$; $T_{S'i}$)-point scatter plot demarcated by asymmetric V(-2,5)-TC at $T_{out}\in$[-3,5; -2,5] and V(-5,5)-TC at $T_{out}\in$[-6,5; -5,5] showed a relatively large fluctuations of temperature, T_S, with the scattering amplitude ">20^0C", while outdoor temperature, T_{out}, could change within 1-centigrade TC base-interval. It has been estimated by Kolmogorov-Smirnov (K-S) test that the both DH-parameters, T_{out} and T_S, were distributed uniformly along the asymmetric TC base-interval. By the same K-S test was confirmed that, however, temperature fluctuations along the asymmetric TC contiguous-interval were distributed normally like random variable.

Conclusions

Correlation analysis of stochastic district heating (DH) processes allows discover latent functional dependencies between weather conditions, on the one hand, and DH-system's energetic or hydraulic parameters, on the other hand. Hence the pair correlation between outdoor and supply water temperature, T_{out}&T_S, plays a special role as the most important DH-system's energetic parameters for heat load predictions. The input data set treated here contained DH-parameters', T_{out}&T_S, time series {$T_{out'i}$} and {$T_{S'i}$} including the whole heating season (HS) from October till April. DH-system parameters' T_{out}&T_S functional dependence has been built-up as a regression model for ($T_{out'i}$; $T_{S'i}$)-point scatter plot obtained from corresponding time series {$T_{out'i}$} and {$T_{S'i}$}. In addition to well known linear least squares parametric regression that is by far the most widely used modeling method to fit a mathematical model to experimentally obtained data new temperature contour (TC) approach has been developed as powerful tool for building-up non-parametric regression models. TC in T_{out}&T_S–coordinates is defined as object having simultaneously both geometrical and statistical properties. TC geometrical properties as width, height, or geometrical centre (GeC) have been estimated using MIN&MAX values and range of ($T_{out'i}$; $T_{S'i}$)-point coordinates surrounded by TC while TC statistical properties as statistical centre (StC) and central tendencies are defined as mean, median and mode of the same ($T_{out'i}$; $T_{S'i}$)-point data set. The most important feature of TC approach is a possibility to split large ($T_{out'i}$; $T_{S'i}$)-point data set belonging to the whole HS, i.e., HS-TC into smaller portions, namely, into an array of subsequent sub-TC_i and build-up partial regression models on the basis of StC_j-points providing effective investigation of the functional dependence between T_{out}&T_S .

Acknowledgements

This research work has been partly supported by DH Company 'Rīgas Siltums' supplying experimental data and having interest in results achieved. Author (U.Kanders) appreciates the interest and valuable discussions with Prof. D.Turlajs and Prof. N.Zeltins concerning heat transmission in DH processes.

References

1. Kanders U., Turlajs D. (2009) Building regression models of district heating processes using temperature domain method. Available at: https://regtransfers-sth-se.diino.com/download/kanders/DiinoSciPapers/Physics/Ortus/UK_DT%27DH-TempDomain_RegrModels.pdf, 09.03.2010.

2. Turlajs D., Kanders U. (2009) Temperature spectroscopy of the district heating processes and building their linear regression models. Available at: https://regtransfers-sth-

se.diino.com/download/kanders/DiinoSciPapers/ Physics/Ortus/UK_DT%27DH-Temp%27FDF_Spectra.pdf, 09.03.2010.